Surface & Coatings Technology 446 (2022) 128816

Contents lists available at ScienceDirect

Surface & Coatings Technology

journal homepage: www.elsevier.com/locate/surfcoat

Water and oil repellent coating on fabric using hollow cathode PECVD

R.G. Mbamkeu Chakounté [a,*], J. Jolibois [b], O. Kappertz [a], J. Chambers [c], H. Weis [b], H. Wiame [d], W. Viöl [a]

[a] Univ Appl Sci & Arts, Fac Engn & Hlth, Von Ossietzky Str 99, D-37085 Göttingen, Germany
[b] AGC Interpane Demonstration and Research Center, Sohnreystr 21, 37697 Lauenförde, Germany
[c] AGC Plasma Technology Solutions, 9881 Horn Road, Suite F, Sacramento, CA 95682, United States of America
[d] AGC Plasma Technology Solutions, Rue L. Blériot 12, 6041 Gosselies, Belgium

ARTICLE INFO

Keywords:
Low-pressure
Hollow cathode
Plasma polymerization
Water and oil repellent

ABSTRACT

Thin film deposition is a suitable process for textile finishing at a time when environmental protection is a global concern. Thin film technology for textile treatments does not only avoid the harmful chemistry and resulting hazardous waste of the wet chemistry, but limits the use of chemicals, water, etc., and do not require a drying system, resulting in a much lower energy consumption. The hollow cathode plasma enhanced chemical vapor deposition is one of the alternatives developed to overcome the wet processings disadvantages. Water and oil repellent finishes are applied through plasma polymerization of short chain perfluoroalkyls precursors. The key advantages of this technology are a high deposition rate and a good uniformity over large areas. However, hollow cathode is a high-density plasma source, appropriate for the deposition of inorganic layers, typically SiO_2, but challenging for the deposition on fabrics without modifying their bulk properties or damaging their surface.

In this work, we demonstrate the successful use of the hollow cathode technology to impart water and oil repellent properties on polyolefin textiles with fluorinated and silicone precursors. The effect of parameters such as power, pressure, gas composition and flow on water and oil repellency have been evaluated according to international standards, water contact angle and the film composition analysed through FTIR measurements. Water contact angles greater than 150°, i.e. superhydrophobic surface, and oil repellency grade of 4 have been obtained.

1. Introduction

Plasma treatments have emerged as promising alternatives to the conventional wet processing of textile to achieve properties such as anti-felting, hydrophobicity, oleophobicity, antibacterial, flame-retardant, anti-soiling [1]. Water and oil repellency are one of the most common functional properties imparted to protective clothing. Mechanical processes change the bulk properties of the treated fabrics [2]. Chemical processes include dip coating, spray coating, the pad-dry-cure method, the sol gel method, the chemical vapor deposition (CVD) and the physical vapor deposition (PVD). The wet chemical processes do yield water and oil repellency [3,4,5,6,7,8] but they go along with a series of inconveniences: in addition to the required monomer that imparts water and oil repellency, they require the use of other complex and toxic chemicals. The processes can last from many hours to many days, must be carried out under high temperatures with large amounts of water. During chemical vapor deposition (CVD) and physical vapor deposition (PVD), coating materials are vaporized through chemical processes in CVD or physical processes in PVD, then deposited on the substrates. This reduces the amount of water needed for the processes, but higher temperatures than in the chemical wet processes are needed [9,10]. Moreover, PVD requires an annealing time in addition to a low deposition rate.

In our study, we propose the impartment of water and oil repellency on fabrics through the hollow cathode plasma enhanced chemical vapor technology, to overcome the problems faced with the previous technologies. The hollow cathode exhibits numerous advantages as cited in [11]. In addition, it was found that a hollow cathode with a large cavity exhibits higher electron densities than a capacitive coupled plasma (CCP) during the deposition of microcrystalline silicon thin films [12], and that a better uniformity can be achieved with an adequate geometry of the hollow cathode [13,14]. As introduced by Yasuda and studied by many others researchers, the polymerization process follows a specific approach, the Quasi-Arrhenius approach [15,16]. It was found that only

* Corresponding author.
E-mail address: rina.chakounte@stud.hawk.de (R.G. Mbamkeu Chakounté).

https://doi.org/10.1016/j.surfcoat.2022.128816
Received 6 May 2022; Received in revised form 29 July 2022; Accepted 18 August 2022
Available online 23 August 2022

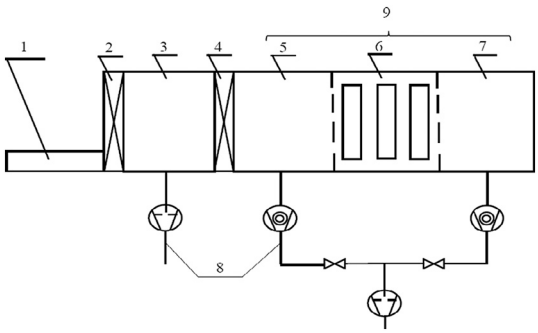

Fig. 1. Vip 1200 coating system.
1. Infeed station, 2. Outer flap, 3. Lock chamber, 4. Inner flap, 5. Buffer chamber, 6. Coating chamber, 7. Overflow chamber, 8. Pump system, 9. Deposition module.

Table 1
Process parameters.

Monomer	Gas	Power (kW)	Speed (m/min)
C_6FA	Ar/O_2, Ar, $Ar/O_2/He$, ArO_4/Ar	0.25 – 1	1 & 2
c-C_4F_8	N_2/He, Ar/He, Ar	0.9 – 1.8	2
TMDSO	$Ar/O_2/He$, Ar/O_2, N_2, N_2/H_2, N_2/He, Ar/He	0.875 – 2.5	0.3–1
HMDSO	Ar/He, N_2/He, Ar/N_2, Ar/O_2, O_2	1.8 – 2.2	0.3

the parameter W/FM controls the conversion of the monomer to the plasma polymer [17]. Concerning hydrophobicity, the highest contact angles are obtained when W/FM is equal to apparent activation energy determined by the slope of the linear fit of the Quasi-Arrhenius plot [18]. A wide range of monomers can be used with this technology for hydrophobicity and oleophobicity, among which hydrocarbons, fluorocarbons, silicones. Silicones such as HMDSO, TMDSO are well known to impart only water repellency on fabrics, since their energy is lower than that of water and higher than that of oil. On the other hand, fluorocarbons can be used for both applications [19]. Within fluorocarbon, short chain monomers are gaining more attention, because they are not expected to break down in the environment into perfluorooctanoic acid (PFOA) and (perfluorooctane sulfonate) PFOs like the C_8 based monomers.

In this work, the hollow cathode plasma technology was used to impart water and oil repellent properties on polyolefin textiles using HMDSO, TMDSO c-C_4F_8 and a C_6 based monomer. The effect of parameters such as power, pressure, gas composition and flow on water and oil repellency have been evaluated according to international standards, contact angle and the film composition analysed through FTIR measurements. We found that HMDSO provides a better water repellency than other precursors, with a water contact angle of more than 150°. The C_6 based monomer provides water and oil repellency and has a better durability than other monomers.

2. Experimentals

The industrial coater used for plasma polymerization via HC-PECVD, named Vip 1200 is represented by Fig. 1. It consists of a 3.6 × 2.4 mm process chamber made of magnetron cathodes and stainless-steel sheets anodes to create a dense plasma around the outlet of the cathodes and around the gas inlets. The whole is equipped with two molecular pumps. For the experiment the reactor was driven with a frequency of 20 Khz.

The coating experiments were conducted in two steps: an oil repellent coating with fluorine using C_6FA on PES#1 fabric and c- C_4F_8 on PES#2 fabric as monomers, then a fluorine free water repellent coating using TMDSO and HMDSO on PES#2 fabric as monomers. All the samples were washed before coating, to remove impurities. PES#1 samples were coated without plasma pretreatment while the PES#2 samples were pretreated at 1.8–2.5 kW with different gases and mixtures thereof. The process parameters are summarized in Table 1. The deposition process took place in the process chamber, where the samples were introduced after being placed vertically on a moving carrier. They were then sputtered with the fragmented precursors. The precursors were purged into the plasma through an evaporator.

2.1. Surface characterization of the coated fabric

2.1.1. Oil repellency test

The oil repellent test was carried out according to the international standard ISO 14419. Test fluids used for this standard are harmful, so alternative test fluids were used. The new test fluids are derived from the ISO 23232 standard. The table containing the alternative test fluids used are found in Appendix A.

2.1.2. Resistance to surface wetting test

The resistance to surface wetting or spray test was conducted according to the standards ISO 4920 (2012) on textile fabrics and AATCC test method 22 (2005). The test was done using a standard spray rating tester and was performed on 20 × 20 cm samples. For this test, the repellency grade ranges from 0 to 5, where grade 0 means a complete wetting of the entire sample face and grade 5 means no sticking or wetting of the sample face. It is performed by mounting the test sample securely in the hoop of the tester in such a way that the fabric will be exposed to the spray. Then 250 mL column of distilled water is poured into the funnel and allowed to spray for 25 to 30 s.

2.1.3. Water contact angle

The water contact angle was measured by the drop shape analyzer DSA100 device from Krüss. All the measurements were done using distillated water in static mode of the sessile drop method. The contact angle values were obtained by averaging four measurements done on different parts of the same sample measuring 20 × 10 cm.

2.1.4. FTIR

The structure of the coating was analysed by means of a Fourier Transform Infrared spectroscopy (FTIR) using the Invenio R from Bruker. For the analysis, low-e glass samples were coated along with the textile samples. This is because uncoated glass completely absorbs IR radiation, thus does not give a reliable result. Low-e glass has a flatter surface as a textile fabric, this limits scattering from the surface. Low-e glass being a solid sample, there is no need to apply pressure on it to perform the analysis, so we avoid damage.

2.1.5. Thickness measurement

The thickness measurement was done with 10 × 10 cm ordinary glass pieces, using a nano step profilometer. This is because the thickness deposited on fabric surface is expected to be lower than glass due to absorption. However, glass gives good indication of deposition rate.

2.1.6. Washing procedure of the fabrics

The washing was done using an ISO standard washing machine, into which the samples were introduced with some ballast so as to obtain a load of 2 kg. A weight of 20 g of standard detergent was used for a washing of 45 min at 40 °C with a spinning of 1000. This cycle was repeated 25 times. After washing, the samples were hanged on a drying rack and left do dry at room temperature.

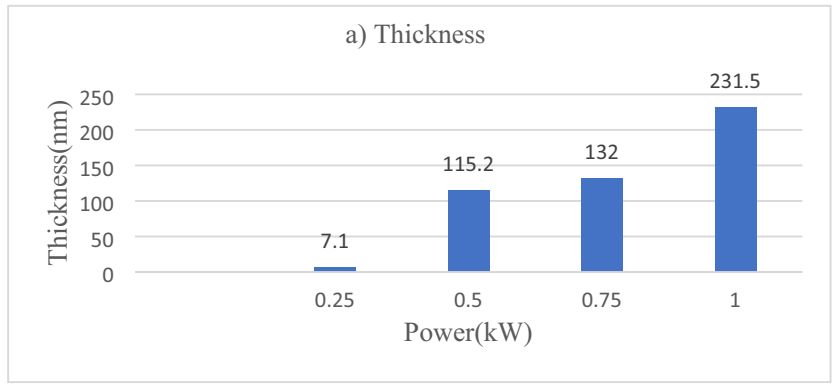

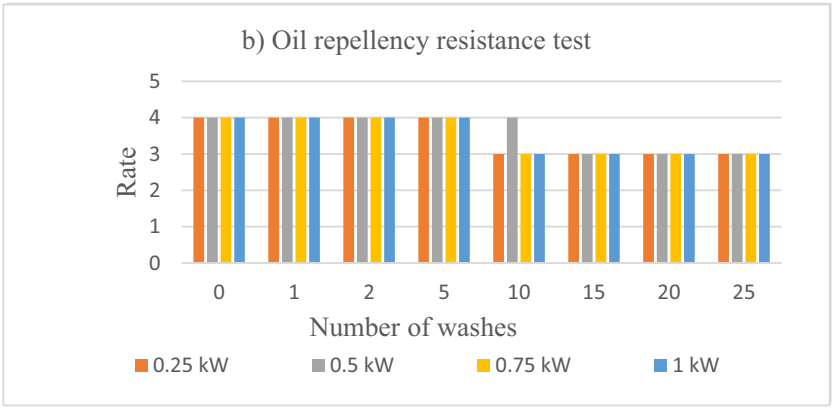

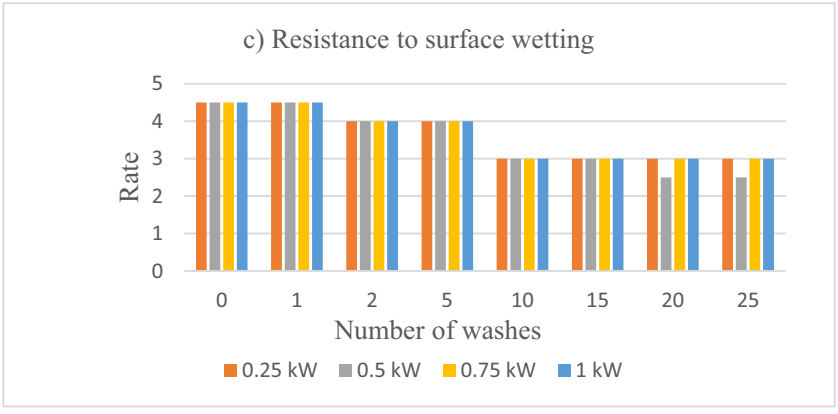

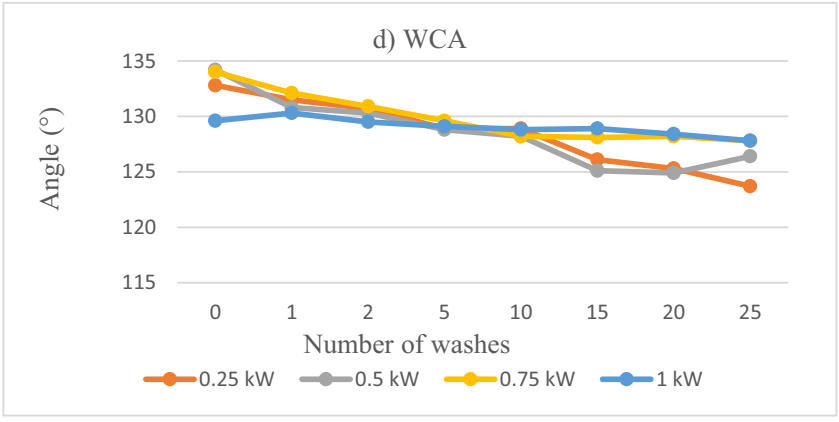

Fig. 2. Power effect (a) Thickness, (b) drop test, (c) spray test, (d) WCA.

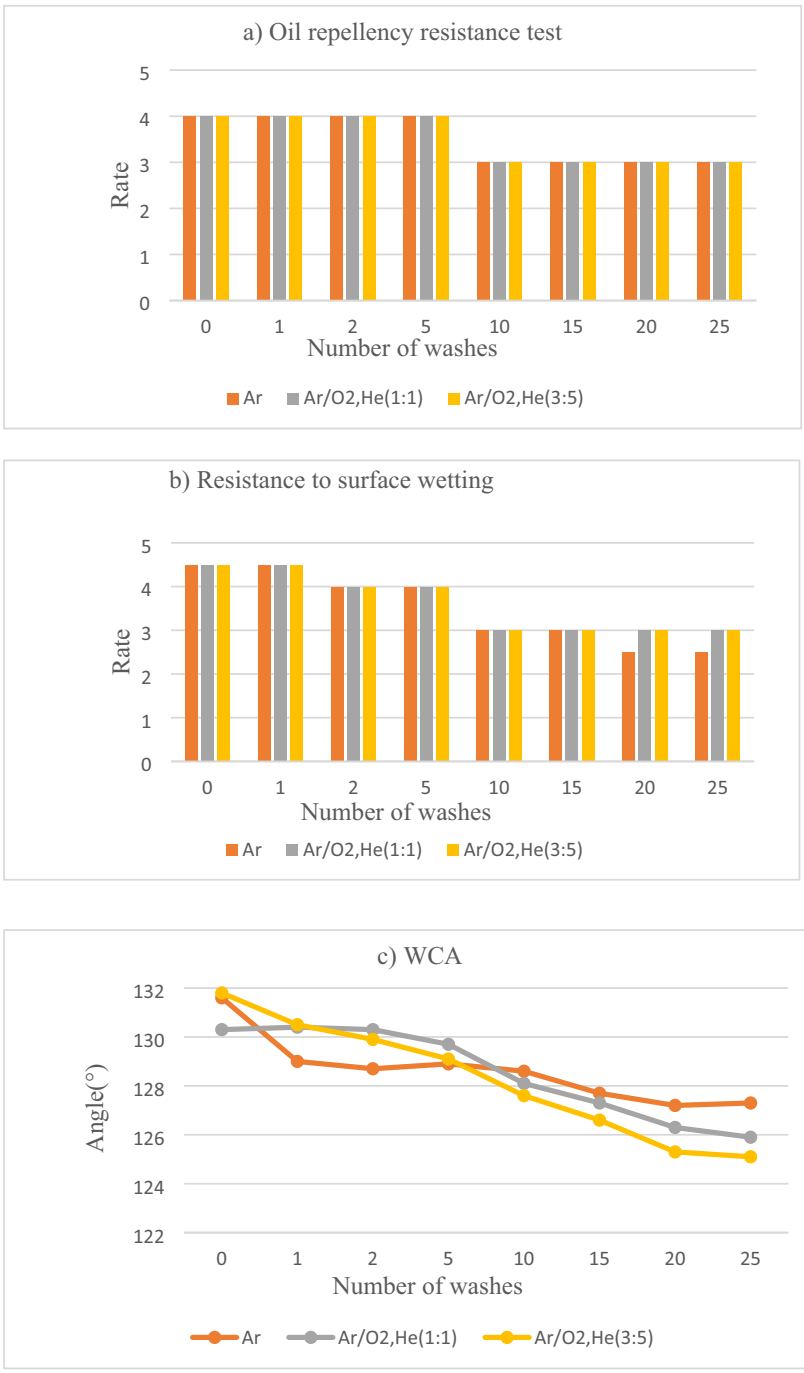

Fig. 3. Effect of gas mixture (a) drop test, (b) spray test, (c) WCA.

3. Results and discussion

3.1. Oil repellent coating

3.1.1. C_6FA

3.1.1.1. Power effect. The results obtained by varying the power show in Fig. 2 that the thickness increases with the power, but at 0.25 kW the deposited layer is too thin: 7.1 nm. Nevertheless, we obtained a very similar rating during the drop test, where after coating and 5 washes the samples were rated at 4, and after 25 washes at 3. The spray test gives a higher rate after coating, that is 4.5, but after 25 washes, the sample coated at 0.5 kW is rated to 2.5 while the others are rated to 3. With the water contact angle, the best values are obtained with 0.5 kW and 0.75 kW. Above 0.75 kW the WCA starts decreasing. The values are around 134° after coating and around 127° after 25 washes.

3.1.1.2. Mixture of Argon Oxygen and He, Ar and Argon Oxygen, comparison with Ar. Performing a coating with pure Ar gives a better thickness than with a mixture of Argon Oxygen and He. The values are 45.3 nm with Ar, 40.7 nm with Argon Oxygen/He (1:1) and 13.6 nm with Argon Oxygen/He (3:5). The values do not influence the rating of the coating regarding the drop test which is at 4 up to 5 washes, then drops to 3 up to 25 washes. The Spray test yields a rating of 4.5 after coating, 4 after 2 washes, 3 after 10 washes. As from 20 washes, we can distinguish a less good performance for samples coated with Ar (rate

Fig. 4. Effect of gas mixture (a) drop test, (b) spray test, (c) WCA.

2.5) than those coated with Argon Oxygen/He. Water contact angle measurements are similar for all the samples, around 130.3–131.8° after coating and 125.1–127.3° after 25 washes. Fig. 3 shows the results obtained by mixing argon oxygen and helium in different ratios and comparing to argon.

On the other hand, the thickness increases with the amount of Ar present in the plasma gas mixture: with a mixture of Argon Oxygen/Ar (2:3) we obtained a thickness of 2.8 nm, with a mixture of Argon Oxygen/Ar(3:5) a thickness of 8.5 nm, with pure Ar and Ar as carrier gas a thickness of 121.1 nm and with pure argon and He as career gas. The performances are similar to that of the previous mixtures, with the difference that the rate given by the drop test is conserved up to 20 washes for samples coated with Argon Oxygen/Ar (3:5) and pure Ar. As for the spray test, samples coated with Ar and He as career gas exhibit the best performance with a rate of 4.5 after coating and 3 after 25 washes. The WCAs are similar for all the samples, in the range of 133.2–135.4° after coating and 126.8–127.5° after 25 washes. These results are illustrated in Fig. 4.

The experimental conditions did not change the composition of the on the PES#1 fabric deposited layer. For all the samples, the following

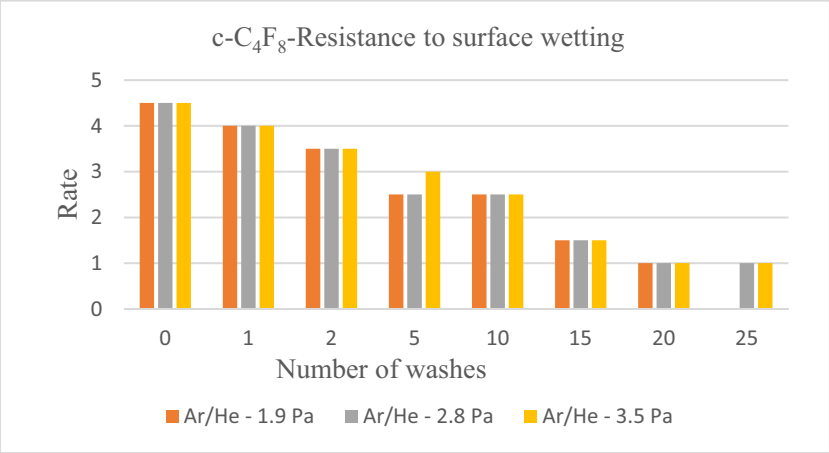

Fig. 5. Resistance to surface wetting for c-C_4F_8.

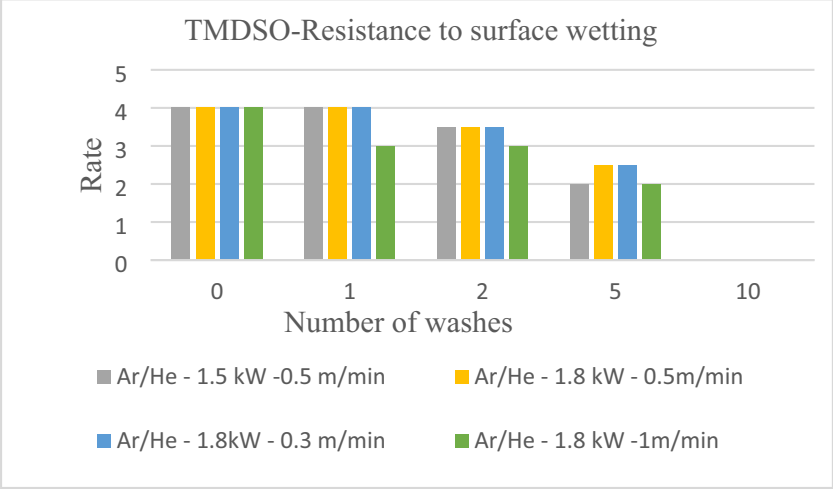

Fig. 6. Resistance to surface wetting for TMDSO.

Table 2
Performances of a few samples coated with HMDSO.

Parameters	Rate	Durability (number of washes)	Thickness (nm)	WCA (°)
100 sccm - Ar/He (2:3) - 1.8 kW	4	15	441.8	142.3
120 sccm - Ar/He (2:3) - 1.8 kW	4.5	15	356.4	146.8
150 sccm - Ar/He (2:3) - 1.8 kW	4.5	15	362.8	145.5
150 sccm -Ar/He (2:3) - 2.2 kW	4.5	15	360.7	150.4
150 sccm - 1.8 kW - He/Ar (1:1)	4.5	10	178.1	150.1
150 sccm - 1.8 kW - He/Ar = 0,67	4.5	10	137.6	151.7
150 sccm - 1.8 kW - He/Ar = 0,67–1,85 Pa	4.5	10	168.4	149.8
150 sccm - 2 kW - He/Ar = 1	4.5	10	311.9	149.8
150 sccm - 1.8 kW - He/N2 = 0.67	3	15	224	145.9

functional groups were observed and showed in Fig. 8: the CF deformation at 630 cm^{-1} [20]. The CF_2 symmetric stretching [20,21] and the C—O stretching at 1150 cm^{-1} [22], the CF_3 stretching [23] and the C—C bond at 1258 cm^{-1} [22], the C═O stretching at 1748 cm^{-1} [24] and the O═C═O stretching at 2352 cm^{-1} [25].

3.1.2. *c-C_4F_8*

For flow rates lower than 150 sccm, samples coated with c-C_4F_8 are only water repellent. The spray test rates them to 2.5, with a water contact angle of 135.7°–137.5°, but the coating is completely removed after the first wash so that the sample become hydrophilic. At 150 sccm, all the samples show water and oil repellency after coating and only water repellency after being subjected to the first wash. What makes the difference between the various experimental conditions is the durability of the water repellency. The best result is obtained by using Ar/He with a ratio of 5:7, or at high pressure: 2.8–3.5 Pa, or with a higher number of passages:24, or with a higher flow. With these parameters, we obtained a rating 4.5 with the spray test which decreased progressively to 0 after 20 or 25 washes. Fig. 5 shows the resistance to surface wetting for the c-C_4F_8 coated samples.We could achieve water contact angles up to 143.9° (Ar/He and 24 passages). Variating the power has no influence on the performance of the coating. We observed no discoloration on the samples after coating.

The FTIR diagram shows the presence of the CF deformation at 629 cm^{-1} [20], the CF_2 symmetric stretching mode at 1231 cm^{-1} [26] and the O═C═O stretching mode of carbon dioxide. The CF_2 is detected with a very low intensity at 150 sccm and is almost not to see under 150 sccm. This could explain why the oil repellent character disappears after

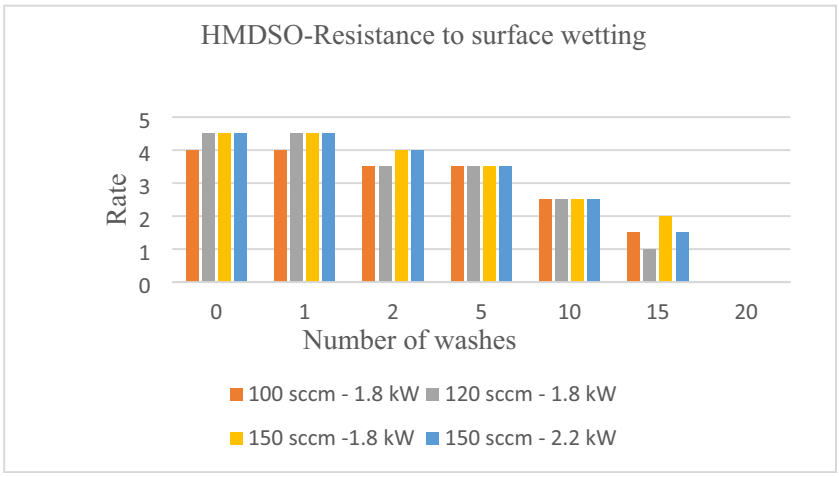

Fig. 7. Resistance to surface wetting for HMDSO.

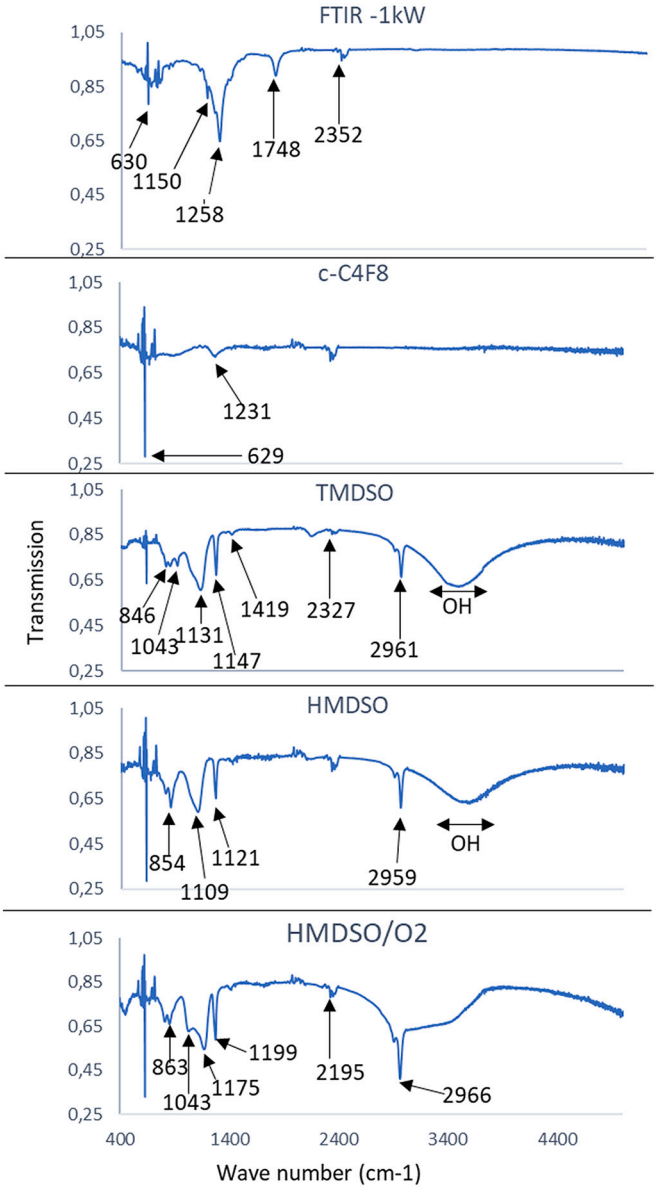

Fig. 8. FTIR for all the precursors.

the first wash. C_6FA coating performs better than c-C_4F_8 for multiple reasons: first, its perfluorinated carbon chain is longer than that of c-C_4F_8, then C_6FA contains an acrylic group than ensures adhesion to the fabric [27]. We also note the F/C ratio which is lower for C_6FA (F/C ratio of 0.67) than for c-C_4F_8(F/C ratio of 2), calculated by the formular given by Li et al. [28]. This shows that C_6FA is more polymerizable than c-C_4F_8. According to research done by Hegemann et al. [18] where the polymerization of a short chain fluorocarbon (hexafluoropropene or HFP) and a long chain fluorocarbon (perfluorodimethylcyclohexane or PFDMCH) is compared, the long chain fluorocarbon is more stable and effective for cross-linking. FTIR shows that the C_6FA coated layer contains more fluorinated groups than the c-C_4F_8 coated layer, which lower the surface energy of the samples [29]. Fig. 8 illustrates the FTIR diagram and the pressure effect of the coating with c-C_4F_8.

3.2. *Fluor-free water repellent coating*

3.2.1. *TMDSO*

The coating with TMDSO leads to water repellent fabrics. The power is the parameter which has more influence on the treatment, when associated with other parameters. At low powers (0.3–1.2 kW), the samples are rated to 3 after spray test, the durability is 10 washes using N_2 at 2.1 kW, with a water contact angle of 134.2° and a layer thickness of 419.2 nm. At high powers (0.875–2.5 kW), the highest rate of 4 with the spray test is obtained when using Ar/He, 1.8 kW and 0.3 m/min or 1 m/min, but the durability is low, 5 washes. The values of the thickness are 693.9 nm at 0.3 m/min and 837.7 nm at 1 m/min. On the other hand, when using N_2, 2.5 kW and 1 m/min or 0.5 m/min, the rate is lower, 2.5 but the durability is longer, 25 washes, although the thickness is lower: 293.3 nm at 1 m/min and 769.3 nm at 0.5 m/min.

The spectrum of TMDSO shows a peak at 846 cm^{-1} corresponding to the Si—C stretching [30]. The Si—O—Si stretching exhibits transmission at 1043 cm^{-1}, 1131 cm^{-1} and 1147 cm^{-1} [31]. The C—H bond is detected at 1419 cm^{-1} [31], the O═C═O stretching mode of carbon dioxide at 2327 cm^{-1} [25], the CH3 symmetric and asymmetric stretching at 2961 cm^{-1} [30] and the OH group exhibits a transmission band approximately between 3358 and 3632 cm^{-1}. The OH group is hydrophilic and contributes to reduce the durability of the water repellency of the samples. Fig. 8 shows the FTIR diagram and Fig. 6 the spray test result at high power with Ar/He.

3.2.2. *HMDSO*

Concerning silicon coating, HMDSO yielded better results than TMDSO in terms of rating and durability. Just like TMDSO, the coating is water repellent. The samples are best rated to 4.5 at 120–150 sccm, Ar/He at a ratio of 2:3, 1.8–2.2 kW with the spray test. When the amount of

Table 3
Comparative study of different methods of water and oil repellent coating on textile.

Substrate	Material	Method	WCA (°)	Water repellency grade	Oil repellency grade	Reference
Cotton	Stearic acid, maleic acid, SHP, TEA	Pad-dry-cure	142	4	1	[3]
Cotton	ZnO/SiO_2	Pad-dry	–	2.5	6	[4]
Cotton	CO/4(SiF-SiQ-SiP)	Sol-gel	135	–	6	[6]
Cotton	Silane, Zr, Ti based nanosols	Sol-gel	149	5	8	[7]
Polyamide	Plasma + C_6 fluorocarbon	Pad-dry-cure	133	5	6.5	[38]
PET	1H, 1H, 2H-perfluoro-1-decene	Plasma	150	–	–	[19]
Cotton	HMDSO	plasma	160	–	–	[39]
PET[TiO2]	C_6 flurocarbon	Plasma+pad-dry	170	5	5	[40]
Polyester-cotton	C_6 fluorocarbon	Spray	132	1	–	[41]
PES#1	C_6FA	Hollow cathode PECVD	135.4	4.5	4	This study
PES#2	c-C_4F_8	Hollow cathode PECVD	143.9	4.5	4	This study
PES#2	TMDSO	Hollow cathode PECVD	134.2	4	0	This study
PES#2	HMDSO	Hollow cathode PECVD	151.7	4.5	0	This study

argon is higher than that of Helium, or when Argon and helium are used in the same amount, the coating is still rated at 4.5, but is less durable. Using He/N2 gives a lower rate of 3 with a durability of 15 washes. The Table 2 shows the best performances obtained with HMDSO.

On the spectrum of HMDSO, the different peaks are detected with a lower intensity than the peaks of TMDSO. The Si—(CH3)n group is detected at 854 cm^{-1} [32], the Si—O—Si bonds at 1109 cm^{-1} and 1121 cm^{-1} [32,33]. At 1121 cm^{-1}, we also found Si—O—C stretching [33]. The O═C═O stretching mode of carbon dioxide is detected in the range 2195–2356 cm^{-1} [25]. The presence of methyl group is indicated by the C—H bond at 2959 cm^{-1} [34]. Finally, the OH bending is detected in the range 3433–3781 cm^{-1} [35].

Compared to TMDSO, the HMDSO coated samples contain an OH band with a lower intensity. This explains why they have a better durability. The plasma gas is the parameter that influences most the water repellency both for HMDSO and TMDSO: by using Ar/He at a power of 1.8 kW, we obtained the highest rate of 4 and 4.5 for TMDSO and HMDSO respectively. With Ar/He as process gas, the same rates can be obtained at 150 sccm for HMDSO, while a higher flow is needed for TMDSO, that is 400–600 sccm. Fig. 8 shows the FTIR diagram of an HMDSO coated sample and Fig. 7 the spray test at high power depending on the flow.

Hegemann et al. [17,36] showed that mixing HMDSO with O_2 supports the film growth during the polymerization by contributing to the radical formation, yielding high deposition rates. Their experiments conducted with a capacitively coupled RF discharge by variating the O_2/HMDSO ratio showed that deposition rates up to 100 nm/min can be obtained with a ratio of 6.7:1. We reproduced this trial with our Hollow cathode: we obtained a dynamic deposition rate of 189.72 nm*m/min with a thickness of 632.4 nm. Despite this achievement, the water repellent coating was poor: the water contact angle was at 140.1° and the spray test at 0. The sample became completely hydrophilic after the first wash, because the addition of O_2 reduces the retention of carbon groups [37]. FTIR also shows a broadened OH band approximately between 5000 and 6000 cm^{-1} (not visible in the current FTIR). Other groups detected are the Si—(CH3)n at 863 cm^{-1} [32], Si-O—Si at 1043 cm^{-1} and 1175 cm^{-1} [32], SiO_2 cm^{-1} asymmetrical stretching at 1199 cm^{-1} [35], O═C═O at 2195 cm^{-1} [25] and CH_3 stretching at 2966 cm^{-1} [35].

The Table 3 below compares this study to a few others using different methods and materials.

4. Conclusion

In this paper, the performance of water and oil repellent coatings on textile fabrics was investigated. This type of coatings can be used for outdoor activities. Among the monomers used for the experiments, only C_6FA exhibits both water and oil repellency with a good durability while silicones exhibit only water repellency. During the coating with C_6FA, the power and gas influence the thickness: the thickness increases with the power, in the presence of a gas mixture, the thickness increases with the amount of Argon present in the mixture. Helium is more efficient as carrier gas than Argon. The highest thickness obtained with C_6FA is 231.5 nm. With c-C_4F_8, the best results were obtained with Ar/He (5:7) or a high pressure (2.8–3.5 Pa) or 24 passages. The minimum flow to obtain oil repellency is 150 sccm. Coating with TMDSO requires high power (0.875–2.4 kW) and a high flow (400–600 sccm) for a good rating of the coating. The best results were obtained for HMDSO with the combination 120–150 sccm, Ar/He (2:3), 1.8–2.2 kW. One of the biggest challenges of this work is to coat the fabrics without discoloring them. This was achieved with by using c-C_4F_8 but is less efficient than C_6FA. Water contact angles higher than 150° were obtained through silicon coating.

CRediT authorship contribution statement

R.G. Mbamkeu Chakounté: Formal analysis, Investigation, Writing – original draft, Writing – review & editing. **J. Jolibois:** Project administration, Conceptualization, Validation, Resources, Writing – review & editing. **O. Kappertz:** Formal analysis, Funding acquisition, Writing – review & editing. **J. Chambers:** Visualization, Writing – review & editing. **H. Weis:** Writing – review & editing. **H. Wiame:** Supervision, Writing – review & editing. **W. Viöl:** Writing – review & editing.

Declaration of competing interest

We wish to confirm that there are no known conflicts of interest associated with this publication and there has been no significant financial support for this work that could have influenced its outcome.

We confirm that the manuscript has been read and approved by all named authors and that there are no other persons who satisfied the criteria for authorship but are not listed. We further confirm that the order of authors listed in the manuscript has been approved by all of us.

We confirm that we have given due consideration to the protection of intellectual property associated with this work and that there are no impediments to publication, including the timing of publication, with respect to intellectual property. In so doing we confirm that we have followed the regulations of our institutions concerning intellectual property.

We understand that the Corresponding Author is the sole contact for the Editorial process (including Editorial Manager and direct communications with the office). She is responsible for communicating with the other authors about progress, submissions of revisions and final approval of proofs. We confirm that we have provided a current, correct email address which is accessible by the Corresponding Author.

Data availability

The data that has been used is confidential.

Acknowledgments

This research was financially supported by AGC Interpane demonstration and research center in Lauenförde, Germany.

Manuela Scholz-Rehling and Dirk Müller are appreciated for the thickness measurements.

Appendix A. Table: oil rating according to the test solution

Oil rating	Standard hydrocarbon	Alternative hydrocarbon
0	None	None
1	White mineral oil	Olive oil (25°)
2	65:35 white mineral/n-hexadecane (Vol)	78:22 water/IPA (25°)
3	n-Hexadecane	70:30 water/IPA (25°)
4	n-Tetradecane	67:33 water/IPA (25°)
5	n-Dodecane	Acetone (10°)
6	n-Decane	Acetone (25°)
7	n-Octane	IPA (25°)
8	n-Heptane	IPA (40°)

References

[1] A.K.R. Choudhury, Principles of Textile Finishing 2017, Woodhead Publishing (Elsevier), 2017, ISBN 978-0-08-100661-0.
[2] L. Naujokaitytė, E. Strazdienė, The effect of finishing upon textile mechanical properties at low loading, Mater. Science 13 (3) (2007).
[3] S.A. Rabia, M. Muhammad, R. Naveed, A. Waqas, H.G. Qutab, Development of free fluorine and formaldehyde oil and water repellent finishes for cotton fabrics through polymerization of bio-based stearic acid with carboxylic acids, Ind.Text. 71 (2020) 145–155.
[4] L. Chirila, D.E. Radulescu, L.O. Cinteza, D.M. Radulescu, M. Tanase, I. R. Stanculescu, Hybrid materials based on ZnO and SiO2 nanoparticles as hydrophobic coatings for textiles, Ind. Text. 71 (4) (2020) 297–301.
[5] M. Hasanzadeh, H. Shahriyari Far, A. Haji, G. Rosace, Surface modification of polyester/viscose fabric with silica hydrosol and amino-functionalized polydimethylsiloxane for the preparation of a fluorine-free superhydrophobic and breathable textile, Coatings 2022 (12) (2022) 398.
[6] J. Vasiljević, B. Tomšič, B. Jerman, I.Boris Orel, G. Jakša, B. Simončič, Novel multifunctional water- and oil-repellent, antibacterial, and flame-retardant cellulose fibers created by the sol–gel process, Cellulose 21 (2014) 2611–2623.
[7] N. Onar, G. Mete, A. Aksit, B. Kutlu, E. Celik, Water- and oil-repellency properties of cotton fabric treated with silaneZr, Ti based Nanosols, Int. J. Text. Sci. 4 (4) (2015) 84–96.
[8] V. Castelvetro, G. Francini, Evaluating fluorinated acrylic latices as textile water and oil repellent finishes, Text.Res J. 71 (5) (2001) 399–406.
[9] Y. Hamedani, P. Macha, T.J. Bunning, R.R. Naik, M.C. Vasudev, Plasma-enhanced chemical vapor deposition: where we are and the outlook for the future, in: Chemical Vapor Deposition - Recent Advances and Applications in Optical, Solar Cells and Solid State Devices, IntechOpen, 2016, https://doi.org/10.5772/64654.
[10] Y. Dietzel, Reaktives Vakuumbogen-Verdampfen und Reaktives Magnetron-Sputtern PVD-Beschichtung von Textilen Oberflächen, available from, https://nbn-resolving.org/urn:nbn:de:swb:14-1103790814484-00373, 2004.
[11] H. Baránkova, L. Bárdoš, Hollow cathode plasma sources for large area surface treatment, Surf. Coat. Technol. 146–147 (2001) (2001) 486–490.
[12] P. Dimitrakellis, E. Amanatides, D. Mataras, D. Rapakoulias, Development of a hollow cathode plasma source for microcrystalline silicon thin films deposition, J. Phys. Conf. Ser. 275 (2011) (2011), 012014.
[13] M. Sugawara, T. Asami, Surf. Coat. Technol. 73 (1995) (1995).
[14] J.R. Chambers, Linearized Hollow Cathode Plasma for PECVD, 60th Annual Technical Conference (TECHCON 2017) SVC, 2017, 2017.
[15] D. Hegemann, Plasma polymer deposition and coatings on polymers, Appl. Surf. Sci. ISSN: 0169-4332 254 (8) (2008) 2499–2505, https://doi.org/10.1016/B978-0-08-096532-1.00426-X.
[16] M. Asandulesa, I. Topala, V. Pohoata, N. Dumitrascu, Influence of operational parameters on plasma polymerization process at atmospheric pressure, J. Appl. Phys. 108 (093310) (2010) 2010.
[17] D. Hegemann, U. Schütz, C. Oehr, RF-Plasma Deposition of SiOx and a-C:H as Barrier Coatings on Polymers, Plasma Processes and Polymers, Copyright _ 2005, WILEY-VCH Verlag GmbH & Co. KGaA, Weinheim, 2005, ISBN 3-527-40487-2.
[18] D. Hegemann, H. Brunner, C. Oehr, Plasma Treatment of Polymers to Generate Stable, Hydrophobic Surfaces, Plasmas and Polymers Vol. 6, No. 4, 2001. December 2001.
[19] N. de Vietro, Plasma treatment for preparing durable water repellent and anti-stain synthetic fabrics for automotive applications, J. Surf. Eng. Mater. Adv. Technol. 2015 (2015), https://doi.org/10.4236/jsemat.2015.53012.
[20] J. Mihály, S. Sterkel, Hugo M. Ortner, L. Kocsis, L. Hajba, É. Furdyga, J. Minka, FTIR and FT-Raman spectroscopic study on polymer based high pressure digestion vessels, Croat. Chem. Acta 79 (3) (2006) 497–501.
[21] V. Kumar, J. Pulpytel, F. Arefi-Khonsari, Fluorocarbon coatings via plasma enhanced chemical vapor deposition of 1H,1H,2H,2H-perfluorodecyl acrylate - 1, spectroscopic characterization by FT-IR and XPS, Plasma Process. Polym. 2010 (7) (2010) 939–950.
[22] A.B.D. Nandiyanto, R. Oktiani, R. Ragadhita, How to read and interpret FTIR spectroscope of organic material, Indones. J. Sci. Technol. 4 (1) (2019) 97–118. April 2019.
[23] V. Balachandran, M.K. Murali, FT-IR and FT-Raman spectral analysis of 3-(trifluromethyl) phenylisothiocyanate, Elixir. Vib. Spec. 40 (2011) (2011) 5105–5107.
[24] I. Kubovský, D. Kačcíková, F. Kačík, Structural changes of oak wood main components caused by thermal modification, Polymers 12 (2020) 485, https://doi.org/10.3390/polym12020485.
[25] X. Feng, C. Matranga, R. Vidic, E. Borguet, A vibrational spectroscopic study of the fate of oxygen-containing functional groups and trapped CO2 in single-walled carbon nanotubes during thermal treatment, J. Phys. Chem. B 2004 (108) (2004) 19949–19954.
[26] I.P. Vinogradov, A. Dinkelmann, A. Lunk, Deposition of fluorocarbon polymer film in a dielectric barrier discharge (DBD), Surf.Coat.Technol. 2003 (2003) 509–514.
[27] S. Xiong, X. Guo, S.Wu. Ling Li, Paul K. Chu, Z. Xu, Preparation and characterization of fluorinated acrylate copolymer latexes by mini emulsion polymerization under microwave irradiation, J. Fluor. Chem. 131 (2010) (2010) 417–425.
[28] C. Li, Gottlieb S. Oehrlein, R. Gupta, V. Pallem, Impact of hydrofluorocarbon molecular structure parameters on plasma etching of ultra-low-K dielectric, J. Vac. Sci. Technol. A 34 (3) (2016). May/Jun 2016.
[29] N. Li, F. Zeng, Y. Wang, D. Qu, W. Hu, Y. Luan, S. Dong, J. Zhang, Y. Bai, Fluorinated polyurethane based on liquid fluorine elastomer (LFH) synthesis via two-step method: the critical value of thermal resistance and mechanical properties, RSC Adv. 2017 (7) (2017) 30970.
[30] A. Kupareva, P. Mäki-Arvela, H. Grénman, K. Eränen, D.Yu. Murzin, Base-catalyzed transformations of tetramethyldisiloxane, Ind. Eng. Chem. Res. 52 (2013) 10080–10088, https://doi.org/10.1021/ie401711b.
[31] X. Deng, A. Yu Nikiforov, N. De Geyter, R. Morent, C. Leys, Deposition of a TMDSO-based film by a non-equilibrium atmospheric pressure DC plasma jet, Plasma Process. Polym. 2013 (10) (2013) 641–648.
[32] M. Yoshinari, T. Hayakawa, K. Matsuzaka, T. Inoue, Y. Oda, M. Shimono, T. Ide, T. Tanaka, Oxygen plasma surface modification enhances immobilization of simvastatin acid, Biomed. Res. 27 (1) (2006) 29–36.
[33] S. Asadollahi, J. Profili, M. Farzaneh, L. Stafford, Development of organosilicon-based superhydrophobic coatings through atmospheric pressure plasma polymerization of HMDSO in nitrogen plasma, Materials 12 (2019) 219, https://doi.org/10.3390/ma12020219.
[34] R. Krumpolec, A. Zahoranová, M. Černák, D. Kováčik, Chemical and physical evaluation of hydrophobic pp- HMDSO layers deposited by plasma polymerization at atmospheric pressure, Chem. List. 2012 (2012).
[35] V. Raballand, J. Benedikt, A. von Keudell, Deposition of carbon-free silicon dioxide from pure hexamethyldisiloxane using an atmospheric microplasma jet, Appl. Phys. Lett. 92 (2008) (2008), 091502.
[36] D. Hegemann, U. Vohrer, C. Oehr, R. Riedel, Deposition of SiOx films from O2/HMDSO plasmas, Surf. Coat. Technol. 116–119 (1999) (1999) 1033–1036.
[37] N.E. Blanchard, V.V. Naik, T. Geue, O. Kahle, Dirk Hegemann, M. Heuberger, Response of plasma-polymerized hexamethyldisiloxane films to aqueous environments, Langmuir 2015 (31) (2015) 12944–12953, https://doi.org/10.1021/acs.langmuir.5b03010.
[38] A. Hedegård, Durable Oil and Water Repellent Outdoor Fabrics by Atmospheric Plasma Treatment: Reducing the Use of Perfluorinated Compounds, 2014 (Master's thesis).

[39] J. Yang, Y. Pu, D. Miao, X. Ning, Fabrication of durably superhydrophobic cotton fabrics by atmospheric pressure plasma treatment with a siloxane precursor, Polymers (Basel) 10 (4) (2018) 460.
[40] E.A. Siddig, Y. Zhang, B. Yang, T. Wang, J. Shi, Y. Guo, Y. Xu, J. Zhang, Plasma-exposed TiO2 nanoparticles on polyethylene terephthalate matrix surface and its effects on the durable hydrophobic coating, Text. Res. J. 92 (13–14) (2022) 2162–2173.
[41] O. Jongprateep, C. Mani-lata, Y. Sakunrak, K. Audcharuk, T. Narapong, K. Janbooranapinij, S. Pitiphattharabun, A. Lertworasirikul, A. Laobuthee, N. Thengchaisri, H. Ajiro, H. Yoshidae, G. Panomsuwan, Titanium dioxide and fluoropolymer-based coating for smart fabrics with antimicrobial and water repellent properties, RSC Adv. 2022 (12) (2022) 588.